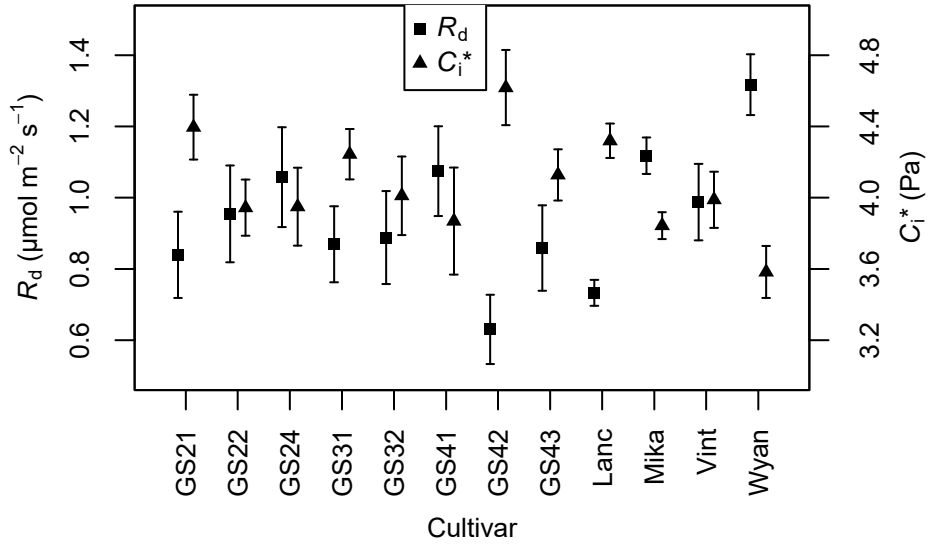


1 SUPPLEMENTARY FIGURES

2

3 **Figure S1.** Mean (\pm s.e.) cultivar non-photorespiratory respiration in the light (R_d) and apparent
4 photorespiratory CO₂ compensation points (C_i^*), determined from Laisk curves on $n=5-8$
5 chamber grown plants.



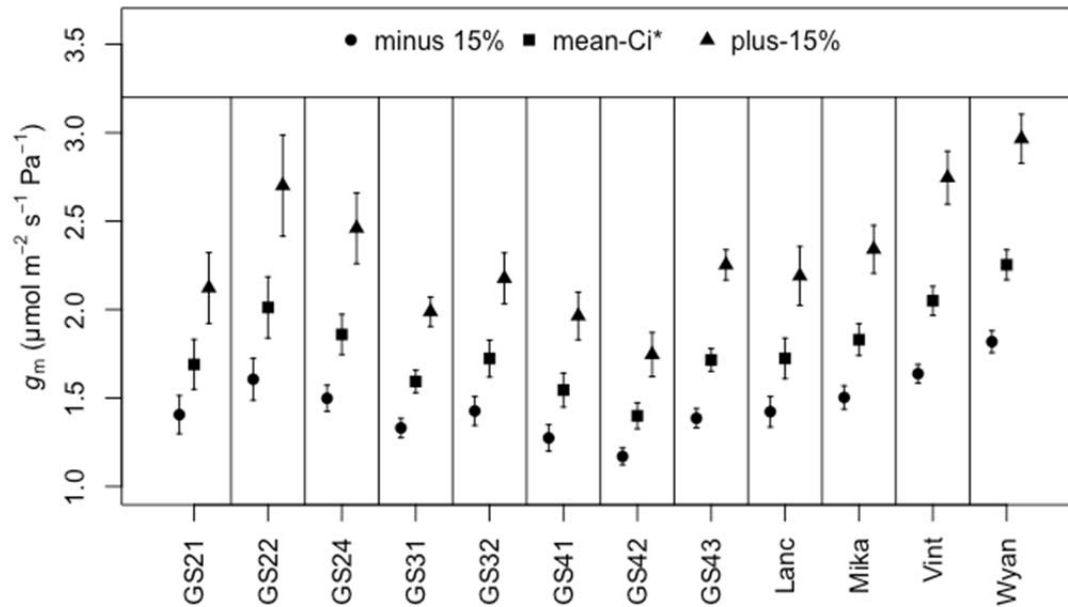
6

7

8

9

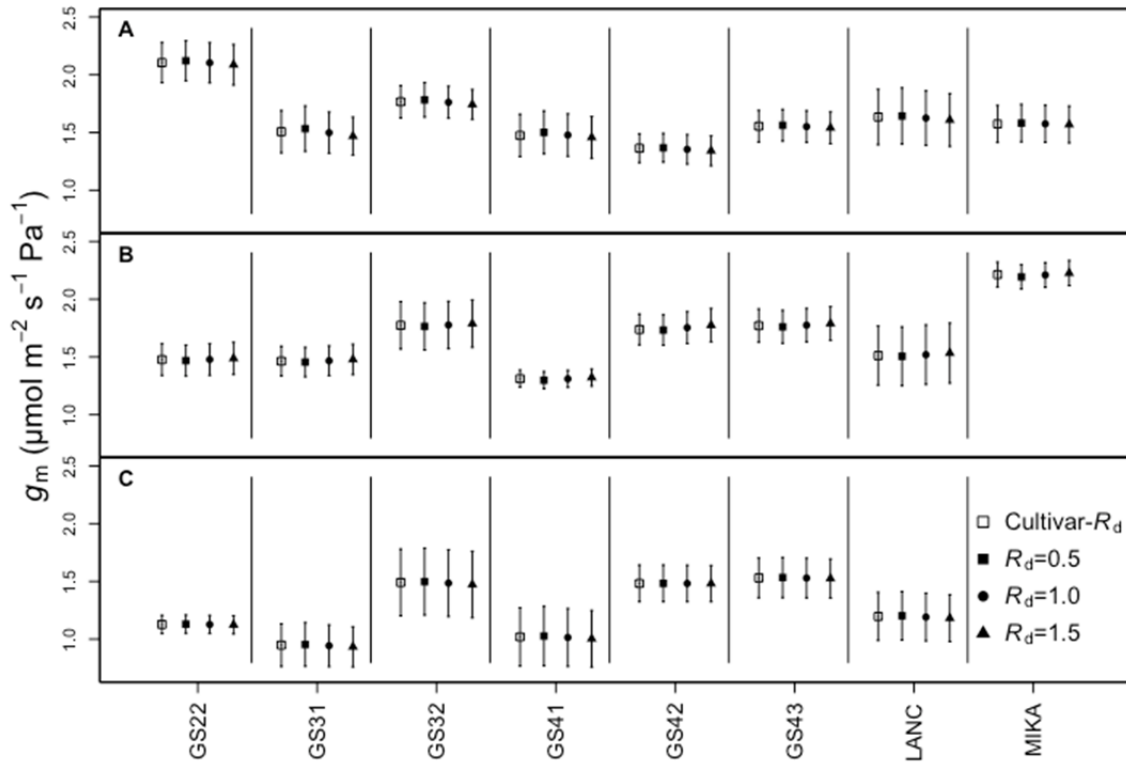
10 **Figure S2.** The reliance of mesophyll conductance (g_m) estimates on the value of Γ^* .
 11 Throughout the manuscript the mean C_i^* value was used as a proxy for the true Γ^* . Here we
 12 varied mean C_i^* by $\pm 15\%$ and re-estimated g_m for all 12 cultivars used in the controlled
 13 environment portion of this study. Mesophyll conductance is strongly dependent on Γ^* ,
 14 increasing with greater values of Γ^* and decreasing with smaller values. Among cultivar
 15 variance in g_m is robust to varying Γ^* : subtracting 15% from the mean C_i^* increases the variance
 16 attributable to cultivar by 0.13% (from 38.81%), and adding 15% to the mean C_i^* decreases it by
 17 1.26%. In all three cases the inclusion of cultivar-identity significantly ($p < 0.05$) increased the
 18 variance explained.
 19



20
 21

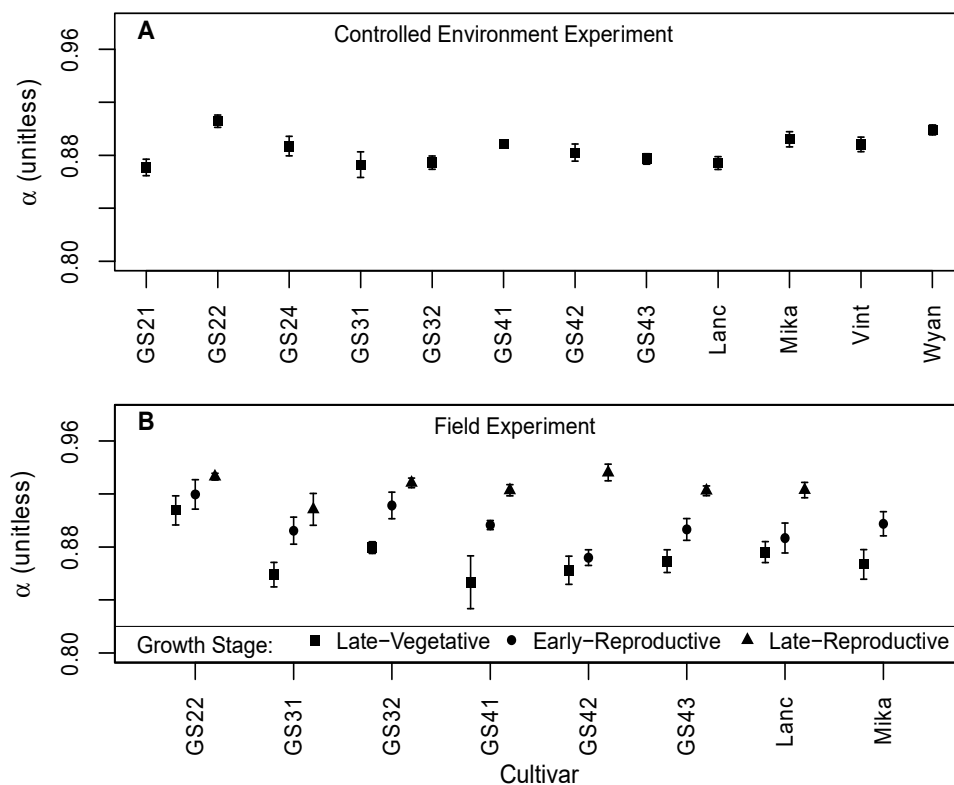
22
23
24
25
26
27
28
29

Figure S3. Comparisons of g_m calculated using cultivar-specific, and a range of unvarying R_d estimates for (A) the late-vegetative, (B) early-reproductive, and (C) late-reproductive growth stages of field grown soybean cultivars indicated along the x-axis. When using cultivar-specific R_d values, 11.6% of the variance in g_m is attributable to cultivar, and when using an unvarying R_d (0.5, 1.0, or 1.5) 11.8% of the variance is attributable to cultivar. The small flux of R_d relative to measured A_N in this study results in g_m being nearly unresponsive to R_d .



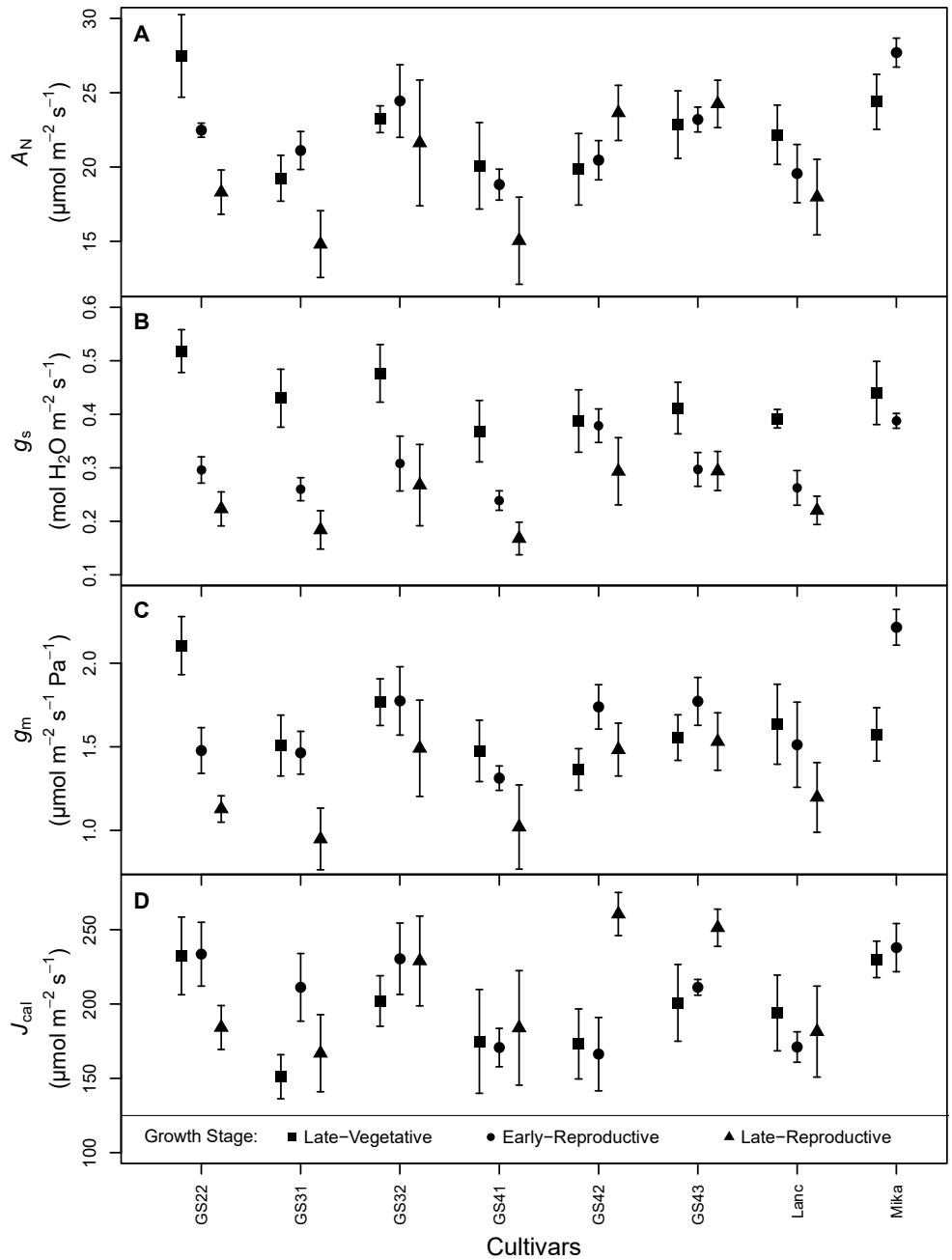
30
31

32 **Figure S4.** Mean (\pm s.e.) absorptance (α) at 470 and 665 nm for each cultivar from the controlled
 33 environment experiment (A) and field experiment (B). In A, $n=5-6$, and in B $n=4$ at each cultivar-
 34 by-growth stage combination except for GS22 where $n=3$. Note all leaves in A were sampled at
 35 the late-vegetative (V₄-V₅) growth stage. In B a mean (\pm s.e.) is presented for each growth
 36 stage measured on each cultivar: squares are late-vegetative, circles are early-reproductive (R₂-
 37 R₄), and triangles are late-reproductive (R₆),
 38
 39



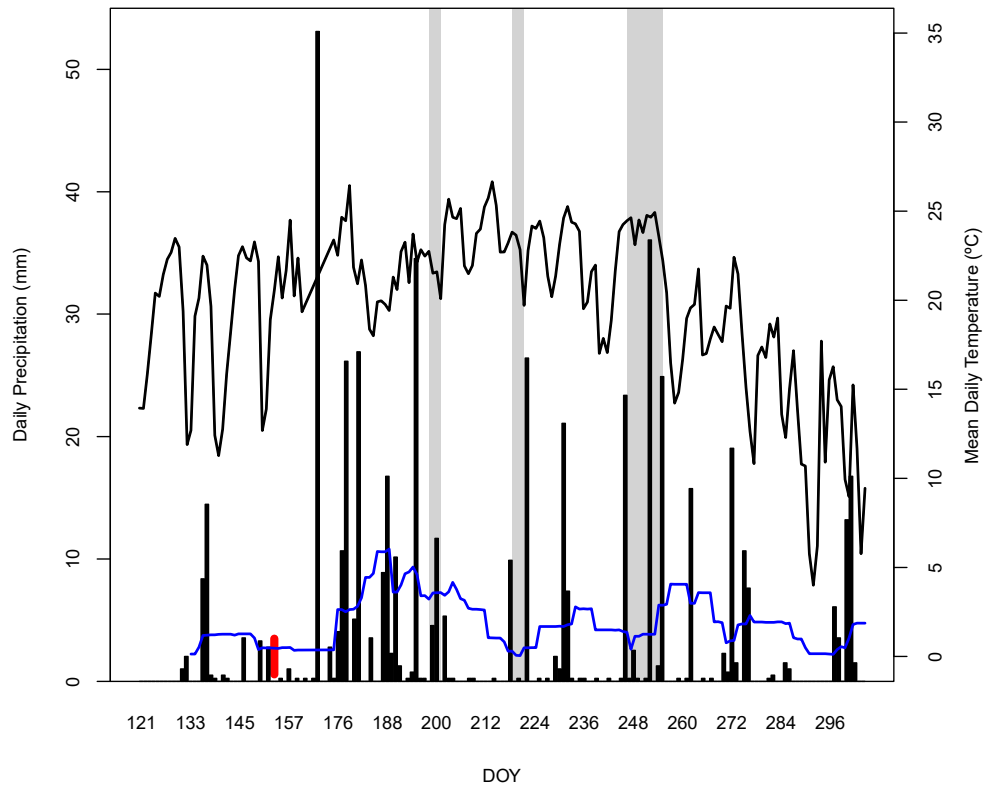
40
 41
 42

43 **Figure S5.** Mean (A) light-saturated assimilation (A_N), (B) stomatal conductance (g_s), (C)
 44 mesophyll conductance (g_m), and (D) calibrated electron transport (J_{cal}) for cultivars grown in
 45 the field. Values are cultivar means (\pm s.e.) for $n=4$ replicates, at the late-vegetative (V₄-V₅,
 46 squares), early-reproductive (R₂-R₄, circles), and late-reproductive (R₆, triangles) growth
 47 stages. Growth stage was a significant fixed effect for g_s and g_m ($p < 0.05$), but not for A_N or J_{cal}
 48 based on linear mixed models with cultivar-identity and row within the field as random effects.
 49 Variance due to cultivar was significant ($p < 0.05$) for A_N , g_s , g_m , and J_{cal} according to likelihood
 50 ratio tests.



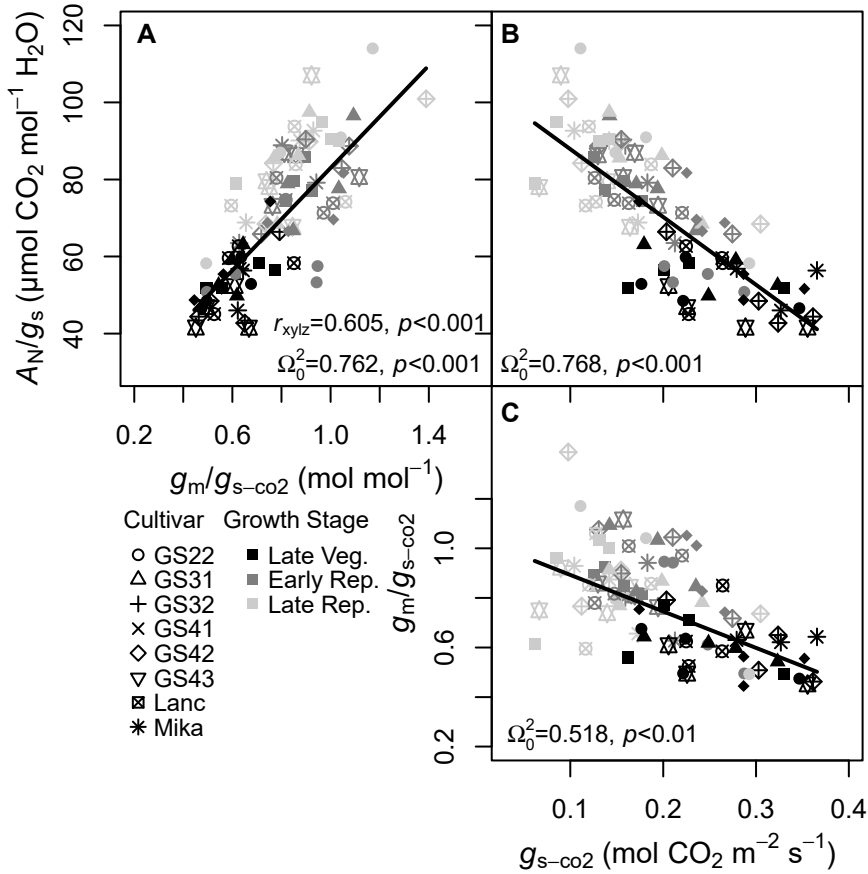
51
52

53 **Figure S6.** Daily precipitation, 15-day cumulative precipitation, and mean temperature across
54 the growing season from a meteorological tower located ~200 m from the field experiment.
55 Mean temperature (black line) was derived from hourly-averaged data. Daily precipitation
56 (bars) represents the cumulative precipitation for each 24-h Julian day of the year (DOY). A 15-
57 day moving window of daily-mean precipitation (blue line) is also presented to highlight wet
58 and dry periods. The red line along the x-axis signifies the date of planting (DOY 155), and the
59 grey shaded regions signify the dates that leaves were sampled and measured. The final
60 measurement date was substantially longer than the first two (two-weeks vs. one) due to
61 blocks reaching the late-reproductive (R6) stage at variable times.



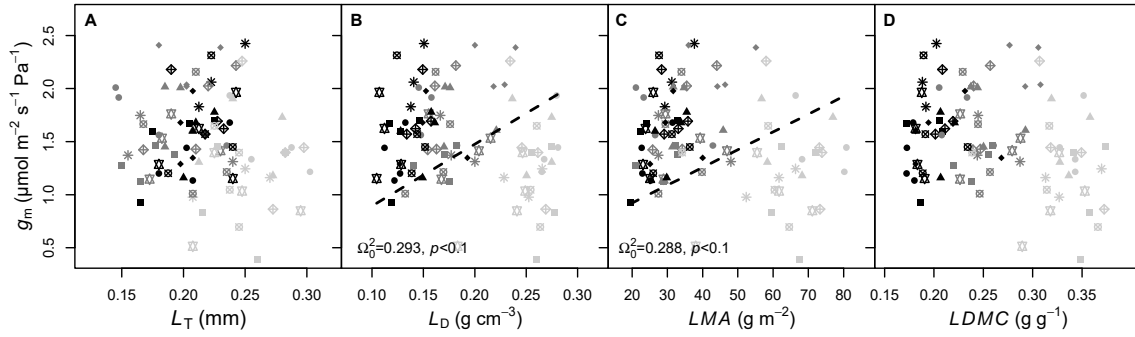
62
63

64 **Figure S7.** Relationship between (A) intrinsic water-use-efficiency (A_N/g_s) and the ratio of
 65 mesophyll to stomatal conductance to CO_2 ($g_m/g_{s-\text{CO}_2}$), (B) A_N/g_s to stomatal conductance to CO_2
 66 ($g_{s-\text{CO}_2}$), and (C) $g_m/g_{s-\text{CO}_2}$ to $g_{s-\text{CO}_2}$. Data are from the eight soybean cultivars grown as part of the
 67 field experiment and measured at three growth stages indicated by symbol shading. Different
 68 symbols represent different cultivars. Coefficients of determination (Ω_0^2) and regression lines
 69 are from linear mixed models with the x-variable and growth stage as predictors, and cultivar
 70 treated as a random effect. In A, the partial correlation (r_{xyz}) of A_N/g_s with $g_m/g_{s-\text{CO}_2}$ after
 71 accounting for g_s is also presented.
 72



73
 74
 75

76 **Figure S8.** Relationships between mesophyll conductance (g_m) and (A) leaf mass *per* area
 77 (LMA), (B) leaf thickness (L_T), (C) leaf density (L_D), and (D) leaf dry matter content ($LDMC$) from
 78 the field experiment. The three growth stages measured were late-vegetative (V_4 - V_5 , black
 79 symbols), early-reproductive (R_2 - R_4 , dark grey), and late-reproductive (R_6 , light grey).
 80 Different symbols represent different cultivars. Coefficients of determination (Ω_0^2) and
 81 regression lines are from linear mixed models with the x-variable and growth stage as
 82 predictors, and cultivar treated as a random effect.



83
 84
 85
 86
 87